An Iodoacetamide Spin-Label Selectively Labels a Cysteine Side Chain in an Occluded Site on the Sarcoplasmic Reticulum Ca^{2+}-ATPase†

Alicja Wawrzynow,‡ John H. Collins,‡ and Carol Coan*,§

Department of Biological Chemistry, School of Medicine and Medical Biotechnology Center, Maryland Biotechnology Institute, University of Maryland, 108 North Green Street, Baltimore, Maryland 21201, and School of Dentistry, University of the Pacific, 2155 Webster Street, San Francisco, California 94115

Received March 2, 1993; Revised Manuscript Received June 17, 1993®

ABSTRACT: Sarcoplasmic reticulum vesicles were labeled with [^{14}C]iodoacetamide spin-label (ISL) under conditions where time courses of the reaction predicted that one amino acid residue would be preferentially labeled. Solubilized tryptic peptides were separated by high-performance liquid chromatography following extensive digestion, and amino acid sequences were determined for major and minor radio-labeled peptides. Only one radio-labeled residue, Cys-674 on the Ca^{2+}-ATPase, could be identified. Extensive incubation with excess label increased nonspecific labeling, but did not produce detectable amounts of any other reactive side chain residue. Time courses of the iodoacetamide spin-label reaction were compared to those of 6-(iodoacetamido)fluorescein (IAF), and the ISL reaction was found to be more selective, in accordance with previous studies showing that IAF labeled both Cys-674 and Cys-670 [Bishop, J. E., Squire, T. C., Bigelow, D. J., & Inesi, G. (1988) *Biochemistry 27,* 5233–5240]. Titrations with spin-broadening reagents $NiCl_2$ and Ni·EDTA showed Cys-674 to be in a region with very low solvent accessibility. These titrations also showed the ATPase to be distributed between two alternating conformations based on the accessibility of the label to $NiCl_2$.

The Ca^{2+}-ATPase of the sarcoplasmic reticulum functions as an ion pump to regulate the Ca^{2+} concentration in the cytoplasm of the muscle cell. A structural model of the enzyme has been derived from the amino acid sequence (Brandl et al., 1986), and it can be said with reasonable certainty that a channel is formed through the membrane by a series of α helices, several of which are connected to large hydrophilic loops that form the site of ATP catalysis. At least one of two Ca^{2+} transport sites is located in the channel (Clarke et al., 1989), a minimum of 45 Å from the ATP binding site (Highsmith & Murphy, 1984; Scott, 1985). The pump is activated when Ca^{2+} binds to the transport sites, initiating changes in structure that allow for the utilization of ATP, and the subsequent transport of the Ca^{2+} [for reviews, see Jencks (1989), Inesi (1992), and MacLennan (1990)].

The means by which Ca^{2+} binding initiates the activation of the enzyme is one of the most important and one of the least understood aspects of the transport mechanism. Certainly, changes in conformation are implicit in the communication between the Ca^{2+} binding sites and the active site, and there is evidence that conformational changes follow Ca^{2+} binding (Dupont, 1976; Champeil et al., 1978; Murphy, 1976; Fernandez-Belda et al., 1984) and the further binding of substrate (Coan & Inesi, 1977; Murphy, 1978; Miki et al., 1981; Imamura et al., 1984; Kurtenbach & Verjovski-Almeida, 1985; Petithory & Jencks, 1986; Suzuki et al., 1987; Lewis & Thomas, 1992). However, this evidence comes mainly from changes in the physical properties of probes or bulk properties of the enzyme, or from changes in the rates of reaction, and the nature of the structural changes that produce these phenomena is not well defined.

In contrast, measurements of fluorescent energy transfer between selectively placed probes have provided concrete information on the folding of the tertiary structure. Investigations of potential changes in the distances between probes have provided evidence of movement of the ATP binding domain toward the phosphorylation site under conditions which would promote phosphorylation (Bigelow et al., 1992). Distances have been determined between IAEDANS,[1] putatively bound to Cys-674 and Cys-670, and FITC on Lys-514 in the nucleotide binding pocket (Squire et al., 1987; Birmachu et al., 1989), between the IAEDANS and the Ca^{2+} sites (Bigelow et al., 1992), and between the IAEDANS and maleimide fluorophores putatively on Cys-344 and Cys-364 (Bigelow & Inesi, 1991). Distances have also been determined between the FITC and the maleimide probes (Bigelow & Inesi, 1991).

It is not coincidental that these distance measurements, and many of the studies on conformational change, involve Cys side chains. There are several reagents which are highly selective for Cys, and among these, those which are derivatives of iodoacetamide have always been found to label a select population. The iodoacetamide derivative that has a spin-label linked to the amide group (ISL) is very sensitive to the conformational change that requires the binding of both Ca^{2+} and substrate to the enzyme, conditions that immediately precede enzyme phosphorylation (Coan & Inesi, 1977; Lewis & Thomas, 1992; Mahaney et al., 1993). The change observed in the EPR spectrum is indicative of a decrease in the rotational motion of the attached spin-label, and this change has been used to help define the binding affinity of Ca^{2+}, as well as to

† This work was supported by the National Institutes of Health Grant GM 38073 and by American Heart Association Grant-in-Aid 880072-40.

* To whom correspondence should be addressed.
‡ University of Maryland.
§ University of the Pacific.

® Abstract published in *Advance ACS Abstracts,* September 15, 1993.

[1] Abbreviations: SR, sarcoplasmic reticulum; FITC, fluorescein 5′-isothiocyanate; ISL, *N*-(1-oxy-2,2,6,6-tetramethyl-4-pipperidinyl)iodoacetamide; IAF, 6-(iodoacetamido)fluorescein; IAEDANS, 5-[[[(iodoacetyl)amino]ethyl]amino]naphthalene-1-sulfonic acid; SDS, sodium dodecyl sulfate; MOPS, 3-(*N*-morpholino)propanesulfonic acid.

0006-2960/93/0432-10803$04.00/0

demonstrate the control of Ca^{2+} on the conformation of the catalytic site (Inesi et al., 1980). In addition, the spectral change has provided one of the few means of monitoring Ca^{2+} binding in the low-affinity state, immediately before Ca^{2+} release into the vesicle interior (Coan et al., 1979). Recently, EPR analysis of the ISL–ATPase spectrum has been used to define a putative role for Mg^{2+} chelation in the utilization of the substrate (Chen et al., 1991).

The use of iodoacetamide derivatives for both conformational studies and distance measurements provides an opportunity for integrating the information obtained from these studies, providing the probes are directed to the same side chains. To date, sites of attachment have been identified for [^{14}C]iodoacetamide and IAEDANS (Yamashita & Kawakita, 1987; Suzuki et al., 1987), and for IAF [5-(iodoacetamido)-fluorescein] (Bishop et al., 1988). In all cases label was found to be on Cys-674, and Bishop et al. (1988) reported IAF to also label Cys-670. The latter researchers also found IAEDANS labeling to be mutually exclusive with IAF, indicating that this probe may also be on Cys-670 (Squire et al., 1987). Both IAF and [^{14}C]iodoacetamide can be detected in trace amounts, making them well suited for peptide analysis, but neither of these derivatives has been used in distance measurements or in conformational studies. IAEDANS has a very weak UV absorbance, making it difficult to detect, and ISL is virtually impossible to detect in dilute solutions. If ISL is also located on Cys-674, or possibly on Cys-670, then the distance from the catalytic site is great (about 45 Å) and the changes in the EPR spectrum associated with phosphorylation may be an indication of major changes in the folding of the large hydrophilic loops. However, as shown below, we do not find ISL labeling to fully block labeling with IAF. Accordingly we have prepared [^{14}C]ISL and have proceeded to isolate the peptides labeled with this derivative. We have also used spectral broadening techniques to look at the accessibility of the labeled site to the aqueous medium so that we may better understand the nature of the site and the changes which follow ligand binding.

MATERIALS AND METHODS

SR vesicles were prepared from the white skeletal muscle of rabbit hind legs using methods previously described (Eletr & Inesi, 1972). Vesicles were stored in a buffered sucrose medium (30% sucrose, 10 mM MOPS, pH 6.8) at 4 °C and were used within 4–5 days of preparation. ATP, phosphoenolpyruvate, lactic dehydrogenase, pyruvate kinase, bovine serum albumin, *N,N'*-dicyclohexylcarbodiimide, 4-vinylpyridine, and ionophore A23187 were purchased from Sigma. ISL [*N*-(1-oxy-2,2,6,6-tetramethyl-4-piperidinyl)iodoacetamide], IAF [6-(iodoacetamido)fluorescein], and tempamine were purchased from Molecular Probes. [^{14}C]Iodoacetic acid was purchased from ICN, trypsin (TPCK-treated) from Worthington Biochemical Co., and DTT from Calbiochem. HPLC-grade acetonitrile (AcCN) and water were obtained from Burdick & Jackson.

Protein concentrations were measured according to the techniques of Lowry et al. (1951) using bovine serum albumin as a standard or were determined from the absorbance at 280 nm using $\epsilon = 1.05$ cm^{-1} for 1 mg of SR protein in 1 mL of 1% sodium dodecyl sulfate (Thorley-Lawson & Green, 1973). These procedures generally agreed to within 10%. ATPase activity was monitored using a coupled assay system with pyruvate kinase (8 μg/mL), phosphoenolpyruvate (1 mM), lactate dehydrogenase (220 μg/mL), and NADH (100 μg/mL) (Anderson & Murphy, 1983). The assay medium contained 10 mM $MgCl_2$, 2 mM EGTA, 2 mM $CaCl_2$, 100 mM MOPS, pH 6.8, 80 mM KCl, 1 μg/mL ionophore A23187, 5 mM ATP, and approximately 10 μg/mL SR.

Synthesis of [^{14}C]ISL. *N,N'*-Dicyclohexylcarbodiimide (final concentration 126 mM) was added to 1 mL of 100 mM [^{14}C]iodoacetic acid in dry acetone. Following a 2-min incubation, tempamine (final concentration 150 mM) was added and the incubation extended to 15 min. Small amounts of particulate material were then removed by centrifugation, and the acetone was removed in a rotary evaporator. The remaining solid material was dissolved in a small volume of water (approximately 200 μL), and the [^{14}C]iodoacetic acid was extracted with ether. The purity was checked by thin-layer chromatography using poly(ethylenimine) cellulose sheets with a running buffer of 0.5 M $LiCl_2$, 20 mM MOPS, and 0.5 mM EDTA. The ratio of radio counts associated with the spin-labeled ISL band to the iodoacetic acid band was 9.5:0.5. In addition, substoichiometric amounts of [^{14}C]-ISL were added to concentrated SR (2 nmol of ISL/mg of protein), and the reaction was monitored in the EPR sample chamber. All the spin-label was converted to an immobilized spectrum which could not be removed with repeated washing, demonstrating that it had been covalently bound to SR proteins. The number of covalently bound spin-labels (determined by spectral integration; standard error approximately 10%) agreed with the number of radio counts, giving further evidence of the absence of radio-labeled iodoacetic acid in the preparation. In addition, this method is extremely sensitive to the presence of residual tempamine, which would have a 100:1 line height ratio to the bound label.

Labeling Procedures. (*A*) *ISL.* In experiments designed to label all reactive side chains, 5 mg/mL SR (approximately 40 μM in reactive cysteine residues) was incubated with 400 μM [^{14}C]ISL at 25 °C and pH 6.8 (100 mM MOPS, 80 mM KCl). When indicated, the time course of the reaction was monitored by placing an aliquot of the reaction mixture in the EPR sample chamber and following the decrease in the signal of the freely tumbling, unbound ISL as the reaction proceeded. To observe the EPR signal of the bound ISL–SR, the reaction was quenched by dilution into 10 mL of cold buffer, and pelleted by centrifugation. This process was repeated twice to remove all traces of free ISL, and the sample was resuspended to give a concentration of approximately 60 mg of SR protein/mL. Further detail of the labeling procedures and spectroscopic measurements can be found in Coan and Keating (1981). When stoichiometric amounts of ISL were to be placed on the SR proteins, ISL was added to a concentrated suspension of SR (approximately 75 mg of protein/mL) so that the final concentration was between 2 and 6 nmol/mg, as indicated. The reaction was followed in the EPR sample chamber until at least 95% of the free signal had been incorporated as bound label. The solution was then diluted into 10 mL of cold buffer and pelleted by centrifugation to remove all traces of free label.

A Bruker ER-200D EPR spectrometer (X-band) interfaced with an ER-422VT variable-temperature control system and an IBM S-9001 computer was used with IBM EPR application software for all experimental measurements and data analysis. In all cases, the spectrum was scanned over a 100-G range with a scan rate of 2 g/s, a time constant of 80 ms, and a modulation amplitude of 2 G for protein spectra and 1 G for free spin-label.

(*B*) *IAF.* A 5 mg/mL SR sample was incubated with specified concentrations of IAF, at 25 °C and pH 6.8 (100

mM MOPS, 80 mM KCl). At specified times 200-μL aliquots of the incubation were quenched in 10 mL of 10 mM 2-mercaptoethanol, pelleted by centrifugation, and resuspended in 1 mL of 50 mM Tris buffer, pH 8.5. SDS was added to solubilize the protein (1%), and the concentration of IAF was determined at 495 nm using $\epsilon = 75\ mM^{-1}\ cm^{-1}$ (Bishop et al., 1988). The protein concentration was determined from the absorbance at 280 nm. IAF has a high lipid solubility, and in spite of the 50-fold dilution, residual IAF was found in the membrane. The fraction of membrane-bound IAF was determined by quenching an aliquot of the incubation mixture within 1–2 s of SR addition. This fraction generally varied between 0.2 and 2 nmol/mg as the IAF concentration in the incubation varied from 0.2 to 1 mM.

With both ISL and IAF, time courses were fit with computer programs (provided by Dr. Alexander Murphy) that use a nonlinear regression algorithm (Bevington, 1969) to fit data to a sum of exponential functions.

Preparation of Soluble Tryptic Peptides. Tryptic digestion was performed in a pH 7.0 solution containing 50 mM NH_4HCO_3, 100 μM $CaCl_2$, and 1 mM DTT. SR vesicles were suspended in this solution, and trypsin was added in a 1:1000 weight ratio of trypsin to SR protein. Incubation took place for 4 h at 37 °C. The resulting mixture was then cooled on ice and centrifuged at 18 000 rpm for 1 h. The supernatant was used for peptide purification, and the pellet was discarded. As estimated from scintillation counting and the absorbance at 214 nm, the soluble peptides in the supernatant contained 78–86% of the protein and 71–85% of the radioactivity present in the original sample. After separation from the pellets, Cys thiol groups in the clear supernatants were alkylated by pyridylethylation: a 10:1 weight ratio of 4-vinylpyridine to peptide was added, and the solution purged with N_2 and capped, and incubated for 1.5 h at room temperature. The sample was then dried overnight using a Savant SpeedVac concentrator prior to purification of peptides by HPLC.

Separation and Purification of Peptides. Separation of the soluble tryptic peptides was carried out using a Waters HPLC system equipped with a 1-mL sample injection loop, two Waters M510 pumps, a waters Model 490E multiwavelength detector, and a Waters m 680 gradient controller. A 4.6 × 250 mm Vydac 218TP54 C_{18} reversed-phase column was used throughout for separation and purification. Two steps of purification were used. In the first step, peptide mixtures were dried and redissolved in 100 mM NH_4HCO_3 (pH 7.5), and injected onto the C_{18} column. The column had been previously equilibrated with 0.1% aqueous trifluoroacetic acid (TFA) as solvent A, and peptides were eluted with linear gradients of solvent B (90% AcCN/0.1% TFA). The gradients were as follows: 0–30% B over 60 min, followed by 30–50% B over 30 min, and finally 50–100% B over 10 min. Peptides were detected by monitoring the absorbance of the eluent at 215 nm. Fractions of 2 mL were collected by volume, and 100-μL aliquots were taken from each fraction for $[^{14}C]$ counting using a Beckman LS 6000IC liquid scintillation counter. Radioactive fractions were concentrated on the SpeedVac and applied to HPLC for the second step of purification, in which the solvents contained 10 mM ammonium acetate at pH 6.5 rather than 0.1% TFA. Linear gradients were as follows: 0–50% B over 45 min and 50–100% B over 10 min. Peptide peaks were collected manually according to their absorbance at 215 nm, and aliquots of each were checked for radioactivity. Radioactive peptide peaks from this second purification step were dried on the SpeedVac and prepared for sequencing.

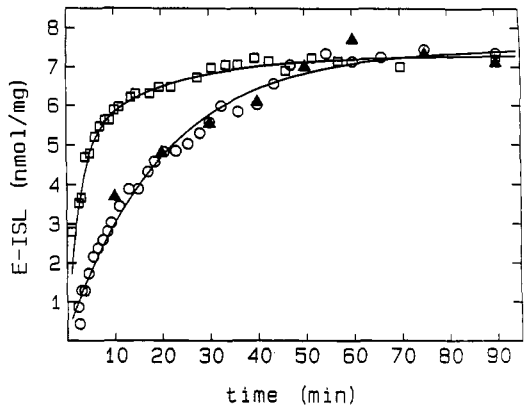

FIGURE 1: Reaction of ISL with the SR ATPase as a function of incubation time. The incubation mixture contained 0.44 mM ISL, 6 mg/mL SR protein, 10 mM $MgCl_2$, and 1 mM $CaCl_2$ (○, ▲) in pH 6.8 buffer (100 mM MOPS, 80 mM KCl), with the addition of 2.5 mM AMP-PCP (□). At the indicated times, the amount of bound label was determined by filtration of SR vesicles and radio counting of $[^{14}C]$ISL (▲), or by monitoring the decrease in the peak to peak amplitude of the free ISL (○, □). Solid lines give best fits to the data with $k = 0.11\ mM^{-1}\ min^{-1}$, [E–ISL] = 7.5 nmol/mg (no substrate), $k_{fast} = 0.9\ mM^{-1}\ min^{-1}$, $[E–ISL_{fast}] = 4.5$ nmol/mg, and $k_{slow} = 0.18\ mM^{-1}\ min^{-1}$, $[E–ISL_{slow}] = 2.8$ nmol/mg (with AMP-PCP).

PAGE was carried out according to Laemmli (1971) on 0.75-mm slab gels (12%) which were then stained with Coomassie blue R250. Before radio counting, the gel was cut in strips and each was dissolved by incubation in 30% H_2O_2 at 60 °C.

Peptide Sequencing. Peptide sequences were determined using an Applied Biosystems Model 477A sequencer equipped with an on-line Model 120A phenylthiohydantoin (PTH) analyzer. The PTH derivatives of ISL-labeled Cys residues were not recovered, but they could be identified by the release of radioactive material. Cys residues that were not labeled with ISL were identified as PTH–(pyridylethyl)cysteine (PTH–PEC).

RESULTS

Reactivity of ISL. Typical time courses for the ISL–SR reaction are shown in Figure 1. In the absence of substrate, the time course could be described by a single population of reactive residues, with a stoichiometry of 7–8 of nmol ISL/mg of SR protein. When AMP–PCP[2] and Ca^{2+} were present, 4.5 nmol/mg reacted at a much faster rate ($k_{fast} = 0.9\ min^{-1}\ \mu M^{-1}$ vs $k_{slow} = 0.18\ min^{-1}\ \mu M^{-1}$, close to the rate without substrate). These results are similar to those obtained in previous EPR measurements (Coan & Keating, 1982; Coan, 1983), but here filtration of the ^{14}C-labeled ISL provides a check on the stoichiometry. Otherwise, the decrease in signal of the free spin-label is followed. The spin-label must be in excess of the enzyme to drive the reaction, and in the latter method the binding stoichiometry is determined from a fairly small signal change (10% in Figure 1). The stoichiometry of the fast reacting residues is close to the maximal levels of phosphorylation of the ATPase, which is usually taken to be 1 mol of ATPase.

Time courses, similar to those in Figure 1, were obtained at several pH values, and as shown in Figure 2, the rate of the labeling reaction increased with increasing pH. Above pH 7.5, the reactivity of the bulk population of Cys residues

[2] AMP–PCP, an ATP analog that cannot be hydrolyzed, is used here. The effect on the labeling reaction and EPR spectrum is the same as that of ATP.

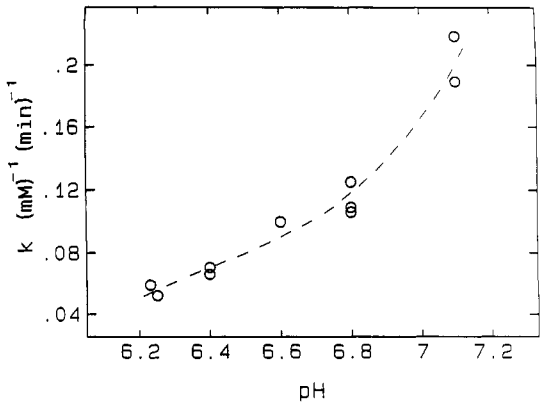

FIGURE 2: Rate of ISL reaction with the SR ATPase as a function of pH. Second-order rate constants were determined from the slope of time courses of the ISL reaction at the specified pH. Reaction conditions and fitting procedures were the same as those used in Figure 1. Substrate was not present in these measurements.

increased and a discrete population of reactive Cys could not be clearly separated. However, the portion of the curve we could obtain indicates that the Cys residues that are most reactive with ISL have a low pK.

Comparative Labeling of IAF. A time course for the IAF reaction with SR is given in Figure 3a. The extent of the labeling is much greater than with ISL, and the time course does not level to the same extent. The overall rate of reaction is lower by an order of magnitude (best fit constants are given in the legend). A time course with SR that had been prelabeled with ISL is also given, and as is evident in the figure, the extent of the labeling is decreased by approximately 4 nmol of IAF/mg of SR protein.

With IAF as with ISL, there is an increase in the reaction rate of about one Cys per ATPase when substrate and Ca^{2+} are present (4.1 nmol/mg from the best fit to data given in Figure 3b). When the ATPase is prelabeled with ISL, the fast reacting population is eliminated, while the remaining population does not appear to be affected.

It should be noted that a relatively high concentration of IAF (1 mM) was used in Figure 3a to improve resolution of the slow reacting population, while a low concentration (200 μM) was used in Figure 3b to better resolve the fast reacting population. However, data were obtained at 200 μM, 400 μM, and 1 mM, under all conditions. The fast reacting population was evident at all concentrations when substrate was present, and the difference due to ISL prelabeling was the same, but both the predicted end point of the time courses and the estimated rate constant increased with the concentration. In theory, this should not happen when the reagent is in an excess of the enzyme, but in practice it is often observed when much slower reacting residues are present. At low concentrations of label, contributions from slow groups can be difficult to detect, although they may reflect the labeling of numerous side chains. As the concentration of the reagent increases, reaction rates increase, and slower labeling groups are more apparent. No appreciable change in the extent of the ISL reaction has been noted with varying ISL concentrations (200–800 μM; Coan & Keating, 1982). This may reflect the 10-fold faster reaction rate of ISL, which would minimize nonspecific labeling during the time course of the reaction if the rate of nonspecific groups did not similarly increase.

While it is clear that the side chains that are sensitive to substrate binding are labeled by both reagents, questions remain as to the relation between the other reactive groups.

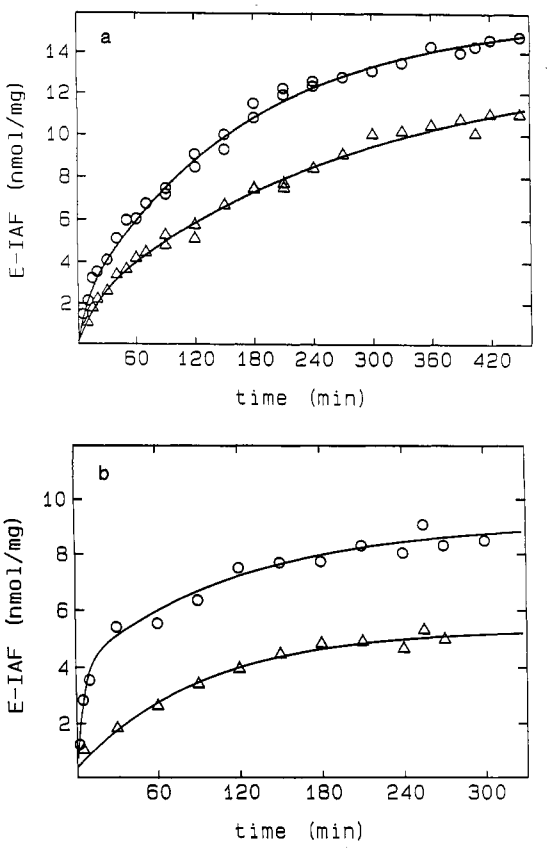

FIGURE 3: Reaction of IAF with the SR ATPase as a function of incubation time. (a) The incubation mixture contained 1 mM IAF, 10 mM $MgCl_2$, 1 mM $CaCl_2$, and 6 mg/mL SR protein using either native vesicles (○) or SR prelabeled with ISL according to the conditions given in Figure 1 (△), in pH 6.8 buffer (100 mM MOPS, 80 mM KCl). (b) The incubation mixture contained 0.2 mM IAF and 2.5 mM AMP–PCP, otherwise as described above. At the indicated times, the amount of bound label was determined from the optical density of IAF at 495 nm as described in the Materials and Methods. Solid lines give best fits to the data. In (a), k = 0.006 mM^{-1} min^{-1} and [E–ISL] = 15 nmol/mg for native vesicles and k = 0.003 mM^{-1} min^{-1} and [E–ISL] = 13 nmol/mg for vesicles prelabeled with ISL. In (b), k_{fast} = 0.95 mM^{-1} min^{-1}, [E–ISL$_{fast}$] = 4.0 nmol/mg, k_{slow} = 0.04 mM^{-1} min^{-1}, and [E–ISL$_{slow}$] = 5 nmol/mg for native vesicles and k_{slow} = 0.05 mM^{-1} min^{-1} and [E–ISL$_{slow}$] = 5.4 nmol/mg for vesicles prelabeled with ISL.

The number of residues protected from IAF labeling by ISL is less that the total number labeled by ISL. The reaction of IAF with Cys-674 and Cys-670 has been reported to be mutually exclusive (Bishop et al., 1988), and this may also be the case with IAF labeling of ISL–ATPase. However, because it is very difficult to bring the IAF reaction to completion (note the time course in Figure 3a was followed for 8 h and the slope was still increasing), it is difficult to make a comparison. When the SR was incubated for over 24 h with IAF and then incubated with ISL, there was no evidence of ISL labeling, but there may also have been enzyme denaturation. A better comparison can be made by isolating the ISL-labeled peptides.

Isolation of [^{14}C]ISL-Labeled Peptides. To selectively place labels on the most reactive thiol groups, aliquots of [^{14}C]-ISL were added to concentrated SR suspensions containing AMP–PCP and Ca^{2+} (Table I). The [^{14}C]ISL concentration varied so that different fractions of the fast and slow reacting populations would be labeled, including one sample in which the SR was prelabeled with non-radio-labeled ISL so that [^{14}C]ISL would be directed to the slower reacting population (sample D). The samples were then subjected to tryptic

Table I: Recovery of Spin-Label from Tryptic Fragments of ISL–ATPase with Varying Degrees of ISL Incorporation[a]

sample	[^{14}C]ISL–ATPase (nmol/mg)	% ISL on fast Cys	% ISL on slow Cys	protein recovery (%)	label recovery (%)
A	2.4	95	5	86	85
B	3.6	90	10	75	75
C	5.4	83	17	75	71
D	2.4	0	100	78	74

[a] The indicated amount of ISL was added to high concentrations of SR (approximately 75 mg/mL or 330 μM) with 3 mM AMP–PCP, 10 mM MgCl, and 5 mM CaCl, and the sample was incubated until all label had been incorporated. The amount of label which was directed to the fast and slow reacting population was calculated from the constants given in Figure 1. In sample D the SR was first incubated with 5 nmol/mg non-radio-labeled ISL. The fraction of recovered protein corresponds to the soluble tryptic fragments (see Materials and Methods).

digestion, and the solubilized peptides were separated by centrifugation (see Materials and Methods). The recovery of radio label closely paralleled the recovery of protein in all samples (about 80%), regardless of the degree of labeling, indicating that the solubilized protein fractionally represented the total label (Table I).

In samples A–C separation of the solubilized peptides by HPLC techniques produced two fractions that contained the majority of the radioactive counts (given as A1, A2, etc. in Table II). In sample D a large portion of the label was spread over many fractions, although two fractions still contained higher than average counts. The separation patterns for samples A and D are shown in Figure 4. The separation patterns for samples B and C (not shown) closely paralleled that of sample A. In each sample the two major fractions were isolated for further purification and sequencing, and in samples B–D, which contained higher levels of radio counts due to the more extensive labeling, additional minor fractions were selected for sequencing. The fractions selected in samples B and C are also indicated in Figure 4a, and the sequencing results for all samples are given in Table II. In all fractions only one radio-labeled amino acid residue could be identified, Cys-674, although in fractions B3 and C3 a specific labeled peptide could not be isolated. In all cases PTH–PEC was found in the Cys-675 position, showing that Cys-675 was not labeled with ISL. The fractions analyzed contained about 80% of the total counts in samples A and B, assuming that the minor fractions were representative (they contained close to the same percentage of counts in each sample).

Fractions B3 and C3 contained multiple peptides, the major peptides that we were able to isolate did not contain Cys or radio counts, and it is quite possible that the small amount of label (about 6%) was spread over several of the minor peptides, making resolution very difficult. However, the lack of identifiable radio-labeled side chains in the major fractions in sample D other than Cys-674 is somewhat surprising considering that this sample had been prelabeled with 5 nmol/mg non-radio-labeled ISL under conditions where most of the reactive side chains should have been labeled. The presence of [^{14}C]ISL–Cys-674 in this sample indicates that this side chain may also comprise some of the slower reacting population. The remaining label is apparently spread to a minor extent over many slow reacting residues.

To determine if some of the labeled side residues were on proteins other than the ATPase (Hidalgo et al., 1978; Lewis & Thomas, 1992), the proteins in a labeled SR suspension (incubated overnight with a 10-fold excess of [^{14}C]ISL) were separated by SDS gel electrophoresis. As shown in Figure 5, 87% of the counts were associated with the ATPase band, 4% were in gel strips on either side that contained little protein, and these counts probably represent trailing or diffusion of the ATPase, and 4% were associated with a narrow protein band above the ATPase, which may be cross-linked ATPase, or another protein. The second of two lower molecular weight protein bands, which are always associated with SR, contained about 2% of the counts, and about 3% were at the solvent front. Strips cut from the rest of the gel contained counts within the error of background measurement.

EPR Spectrum of ISL–ATPase. The EPR spectrum of sample A is shown in Figure 6 with the addition of various

Table II: Sequences of Peptides Containing Radio Label[a]

sample	sequence	radio counts (cpm)	% total cpm	comments
Al-a	AXCFAR	2000	36	single major sequence; X = Cys-674; C = Cys-675
Al-b	AXCFAR			single major sequence
Al-c	AXCFAR			minor sequence
	EVMGSIQLCR			minor sequence (Cys-614)
	IVGGYTCGANTVPY			major sequence, from trypsin
A2	AXCFAR	1150	22	minor sequence
	ALGIVATTGVSTEIGK			major sequence (no Cys)
A3		340	6	sequenced only in sample C3
A4		330	6	sequenced only in sample B3
A5		500	9	sequenced only in sample D3
B1-a	TGTLTTNQMS	2550	47	major sequence
B1-b	AXCFAR			major sequence
B1-c				unidentified mixture; no radio counts or PTH–PEC
B1-d	AXCFAR			minor sequence
	AIYNNMK			major sequence (no Cys)
B3	NDKPIR	510	7	mixture, no detectable Cys or radio counts on major sequence
C1	AXCFAR	4600	28	single major sequence
C2	AXCFAR	1450	9	single major sequence
C3	STTLR	2400	14	mixture, no detectable Cys or radio counts on major sequences
	NDKPIR			
D1-a	AXCFAR	1100	9	minor sequence
	QGIVSWGSGCAQK			major sequence, from trypsin
D1-b	AXCFAR			single major sequence
D2	xxxVGVVGMLDPP	850	8	may be a mixture of two
	AXCF			minor sequence
D3	AXCFAR	640	6	minor sequence, with a mixture of 3–4 unidentified minor sequences

[a] Total = counts in given fraction per sum of counts in all fractions in a given sample; C = PTH–PEC; X = absence of PTH–PEC, radioactive counts; x = unidentified residue.

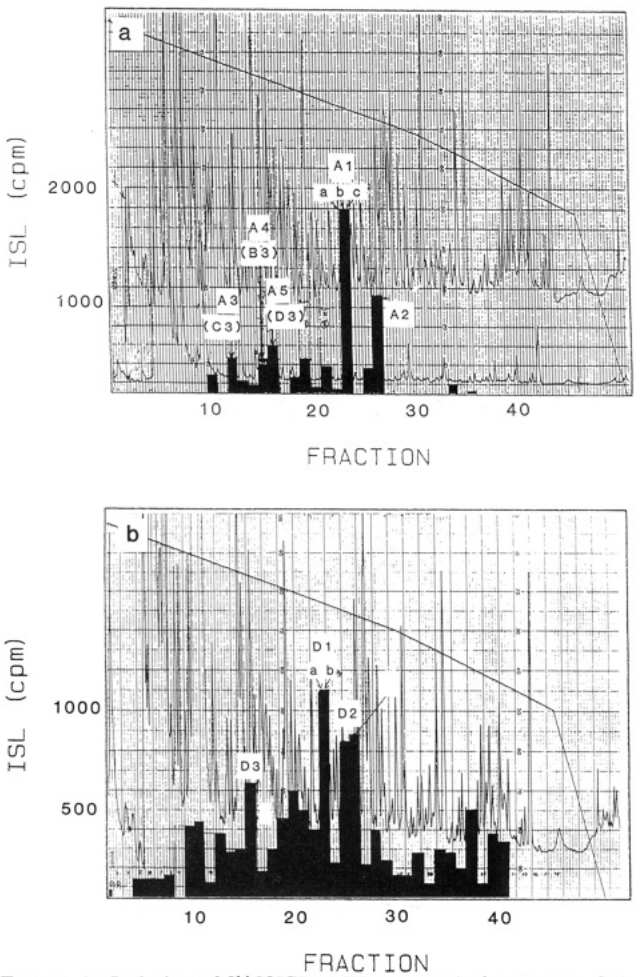

FIGURE 4: Isolation of [^{14}C]ISL–ATPase tryptic fragments. Solubilized fragments of SR proteins, following an extensive tryptic digest, were separated by reversed-phase HPLC as described in the Materials and Methods. Radio counts were determined for each fraction. In (a) the SR was labeled with 2 nmol of [^{14}C]ISL/mg of SR protein in the presence of AMP–PCP and Ca^{2+}. Fractions A1 and A2 were selected for purification and sequencing. Fractions A3, A4, and A5 were sequenced in the indicated samples. In (b) the SR was first labeled with 5 nmol of non-radio-labeled ISL/mg of SR protein, and then labeled with [^{14}C]ISL.

ligands. As with more extensively labeled enzyme, AMP–PCP binding slows down the rotational motion of the spin-label and the addition of Ca^{2+} further restricts the motion (Coan & Inesi, 1977). This is observed in the broadening of the spectral lines and in the increase in the splitting parameter, $2T_{\parallel}$. We also see evidence of a conversion from a one-component to a two-component spectrum when the substrate is removed and then reintroduced. This too is observed with the more extensively labeled enzyme, in terms of both spectral splittings (Coan, 1983) and reaction rates (Coan & Keating, 1982), and can be seen here by comparing the shape of the spectrum shown in Figure 6e (one immobilized component), which was obtained directly from the fast reacting population, to that of the spectrum shown in Figure 6d where the enzyme had been washed and then the substrate added (two components). Lewis and Thomas (1992) have demonstrated that the broadening produced by various combinations of substrate and Ca^{2+} can always be explained by combining the two components in different ratios. Both these observations have been attributed to a shift in the equilibrium between two enzyme conformations, but this interpretation relied on the assertion that predominantely one Cys was labeled (based on the labeling kinetics). In these experiments this appears to be the case.

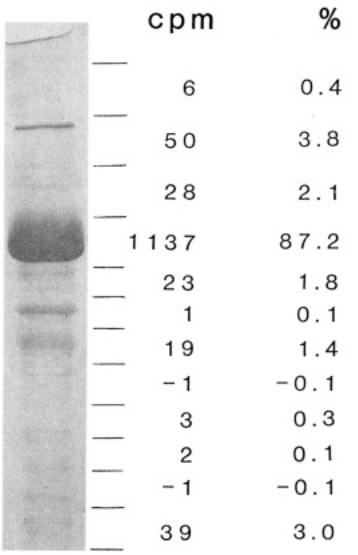

FIGURE 5: Labeling pattern of SR proteins with [^{14}C]ISL. Solubilized SR proteins were separated on a 12% polyacrylamide slab gel. Before solubilization the SR was labeled by incubation overnight with a 10-fold excess of [^{14}C]ISL. The gel was cut into strips and solubilized for counting (see Materials and Methods). Averaged background counts, 40 cpm, were subtracted from the values given in the figure, leading to negative values when given strips counted lower than this background. However, the numerical values of these strips fell within the error of background measurement.

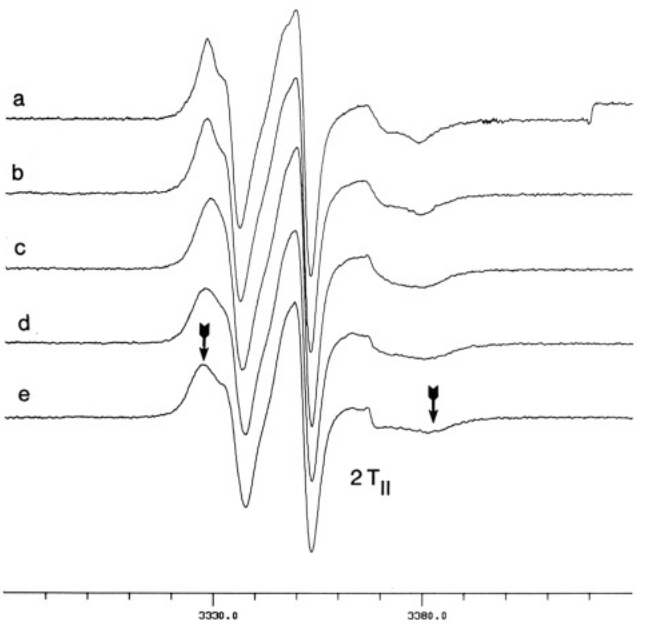

FIGURE 6: EPR spectra of ATPase labeled with a substoichiometric amount of ISL. SR vesicles were incubated with 2.5 nmol of ISL/mg of SR protein until 99%, or more, of ISL signal was converted to the bound form. The medium contained 70 mg/mL SR, 10 mM $CaCl_2$, 10 mM $MgCl_2$, and 2.5 mM AMP–PCP in pH 6.8 buffer (100 mM MOPS, 80 mM KCl). The EPR spectrum at the end of the incubation is shown in Figure 5e. The vesicles were then washed free of ligands from the incubation mixture, and selected ligands were added as follows: (a) 5 mM $CaCl_2$; (b) 5 mM EGTA; (c) 5 mM EGTA and 2.5 mM AMP–PCP; (d) 5 mM $CaCl_2$ and 2.5 mM AMP–PCP. The buffer contained 10 mM $MgCl_2$, 100 mM MOPS, and 80 mM KCl, pH 6.8. The final SR concentration was approximately 40 mg/mL. EPR spectra were obtained with a modulation amplitude of 2 G, 19-mW power, an 80-ms time constant, and a 60-s field scan. Splitting parameters, $T_{\parallel}$, are as follows: (a) 50.7 G; (b) 51.1 G; (c) 50.9 G; (d) 52.4 G; (e) 54.1 G.

The only significant differences between the spectra in Figure 6 and that of the more extensively labeled enzyme is the extremely small change that is observed when Ca^{2+} is

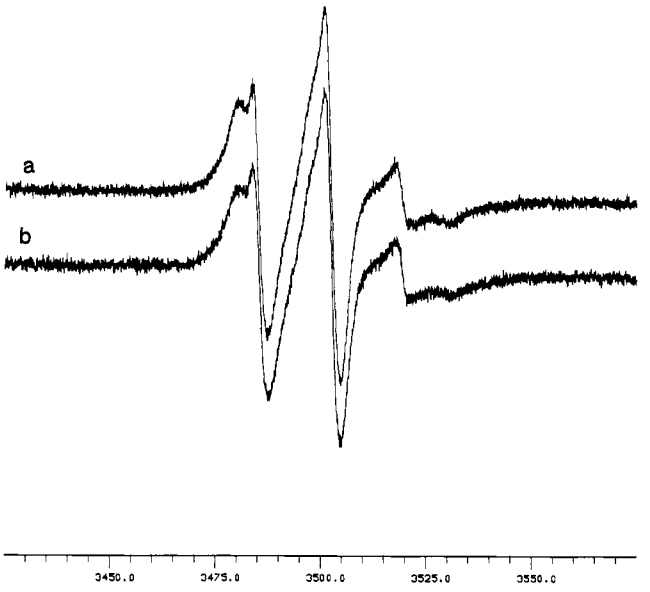

FIGURE 7: EPR spectra of slow reacting side chains. SR vesicles were first incubated with 5 nmol of iodoacetamide (no spin-label)/mg of SR protein under conditions described in Figure 5. The vesicles were then diluted into an ISL medium identical to that described in Figure 1, and incubated for 60 min, and the vesicles were washed and resuspended. In (a), 5 mM $Cacl_2$ was added, and in (b), 5 mM EGTA was added. The buffer contained 10 mM $MgCl_2$, 100 mM MOPS, and 80 mM KCl, pH 6.8. The final SR concentration was approximately 40 mg/mL. EPR spectra were obtained with a modulation amplitude of 2 G, 19-mW power, an 80-ms time constant, and a 60-s field scan. Splitting parameters, $T_{||}$, are (a) 49.8 G and (b) 51.2 G.

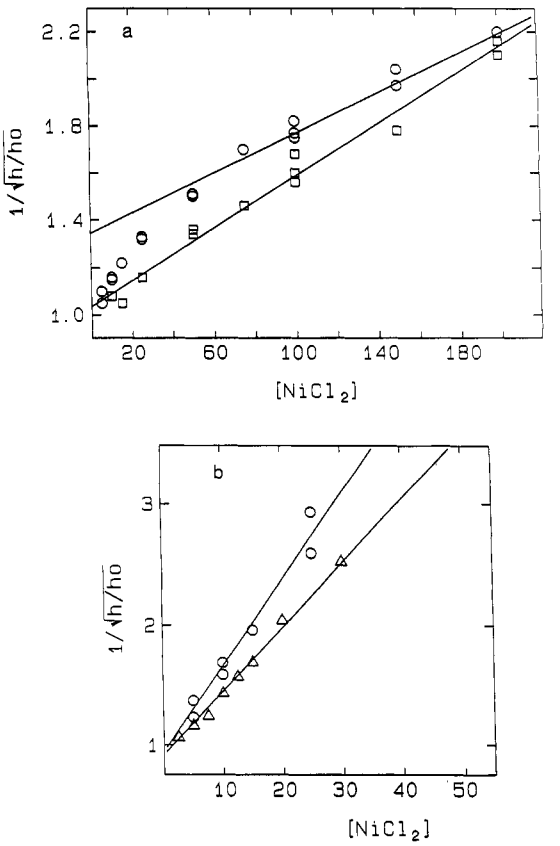

FIGURE 8: Decrease in signal intensity of ISL–ATPase with increasing concentration of $NiCl_2$. The decrease in the peak to peak line height of the center line in the ISL–ATPase spectrum is given as the reciprocal of the square root of the ratio between the line height at a given $NiCl_2$ concentration (h) and before addition of $NiCl_2$ (h_0). (a) (○) With 5 mM $CaCl_2$ in the medium (the slope of the least-squares fit to data points at $[NiCl_2] > 100$ mM is 0.0043); (□) with the further addition of 5 mM AMP–PCP (slope 0.0051). (b) Parameters for the more accessible population of bound ISL (○; slope 0.075) were obtained by subtracting the experimental points given in (a) from the extrapolated least-squares fit to the less accessible population. A titration with free ISL is also given (□; slope 0.053). In all cases the medium contained 20 mg/mL SR (2.5 nmol of bound ISL/mg) (or 200 μM free ISL), 10 mM $MgCl_2$, 100 mM MOPS (pH 6.8), 80 mM KCl, and the specified millimolar concentration of $NiCl_2$.

added without substrate (Figure 1a vs Figure 1b). In fully labeled enzyme Ca^{2+} induces a small, but clearly discernable, increase in the mobility of the labels (Champeil et al., 1978). In the spectra shown in Figure 7, SR was prelabeled with 6 nmol of iodoacetamide/mg of SR protein and then incubated with ISL (as in sample D above), and the increased mobility due to Ca^{2+} binding is quite evident ($\Delta 2T_{||} = 1.4$ G). Apparently the spectra generated by nonspecific sites is more sensitive to Ca^{2+} binding per se than Cys-674, which supports the observation that a fairly globular conformational change accompanies Ca^{2+} binding (Murphy, 1976). The addition of AMP–PCP had a very limited effect on this spectrum.

Availability of Cys-674. When a second paramagnetic species is added to a solution of spin-labeled protein, molecular collisions between the two species will broaden the EPR bands of the labeled protein through Heisenberg spin exchange. If the collisions are random, and there are no additional perturbations, the increase in the width of the EPR bands is proportional to the increase in concentration of the paramagnetic species, with the slope of a titration being directly proportional to the collision frequency (Keith et al., 1977; Yager et al., 1979; Dalal et al., 1985). Although the change in width can be difficult to discern in an anisotropic spectrum if the collision frequency is low, a small increase in width is accompanied by a comparatively large decrease in signal intensity. With an isotropic spectrum, the square root of the peak to peak line height is inversely proportional to the width, and to a first approximation this would be expected to hold for the center line of an anisotropic spectrum (i.e., Figures 8 and 9). Here we have used the decreased intensity to compare the collision frequency of Cys-674 with paramagnetic broadening agents under differing conditions. We have used two broadening agents, Ni·EDTA and $NiCl_2$. Ni^{2+} has a fast relaxation time so that there is no measurable EPR signal under ambient conditions, and there is no evidence of Ni^{2+} binding to the metal sites on the ATPase. EDTA chelates Ni^{2+} very tightly, forming a negatively charged paramagnetic complex with a larger diameter.

The decrease in signal intensity of the ISL–Cys-674 is given as the appropriate function of $NiCl_2$ concentration in Figure 8, and of Ni·EDTA concentration in Figure 9. Under most conditions the expected linear dependency is observed. One exception is the titration with $NiCl_2$ in the absence of substrate (Ca^{2+} present) where there appear to be two populations with considerably different exposures to the cation (Figure 8a). Extrapolation indicates that the less accessible portion constitutes about 50% of the labeled side chains. A titration with AMP–PCP and Ca^{2+} in the medium is also given the figure, and in this case the accessibility of the side chain appears to be uniform. A comparison of the slopes shows the collision frequency to be similar to the less accessible population with just Ca^{2+} present.

In Figure 8b, the concentration dependency of the more accessible population is compared to that of free ISL reagent. The former was obtained by subtracting the extrapolated linear least-squares fit given in Figure 8a from experimental points in the low concentration range. The similarity in slopes

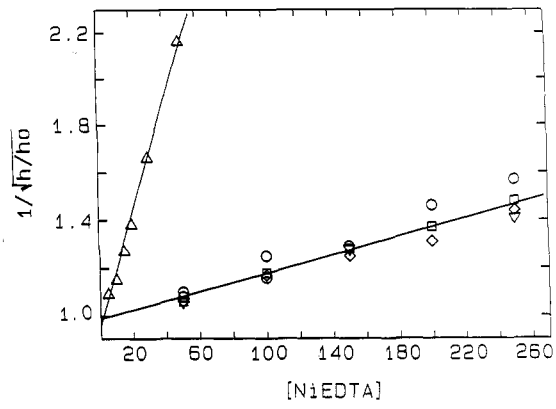

FIGURE 9: Decrease in signal intensity of ISL–ATPase with increasing concentration of NiEDTA. The decrease in the peak to peak line height of the center line in the ISL–ATPase spectrum is given as the reciprocal of the square root of the ratio between the line height at a given NiEDTA concentration (h) and before addition of NiEDTA (h_0). The medium contained 5 mM $CaCl_2$ (○), 5 mM $CaCl_2$ and 5 mM AMP–PCP (□), 5 mM EGTA (◇), or 5 mM EGTA and 20 mM Pi (▽) with 20 mg/mL SR (2.5 nmol of bound ISL/mg), 10 mM $MgCl_2$, 80 mM KCl, and 100 mM MOPS (pH 6.8) (slope to the least-squares fit 0.0019). A titration of free ISL (200 μM) is also given (△; slope 0.023).

indicates that this population of bound probe is fully accessible to the Ni^{2+}. However, consideration should also be given to the possibility that Ni^{2+} binds weakly in the vicinity of the probe. In this case, the line height decrease would be expected to follow the sigmoidal shape of a binding curve, but this difference may be difficult to discern when the decrease is sharp.

When Ni·EDTA is used as a signal broadening agent, the slope of the titration curve is very low (Figure 9). Chelation of a metal by an organic ligand generally decreases the efficiency of a spin exchange (Keith et al., 1977; Dalal et al., 1985), and a titration of free ISL is also given in the figure. By comparing the slope of the free label titration to that given in Figure 8b, it can be seen that the chelation by the organic ligand has decreased the collision frequency by about 30%. When this is taken into consideration, the collision frequency with the Ni·EDTA is similar to that of the less accessible ISL with Ni^{2+}.

An advantage of using Ni·EDTA as a broadening reagent is that the tight binding EDTA allows EGTA to be added to the titration medium to chelate endogenous Ca^{2+} (otherwise EGTA would preferentially chelate Ni^{2+}), so that we can observe the effect of substrate binding in the absence of Ca^{2+}, as well as phosphorylation with Pi. As shown in Figure 9, we found ligand binding not to affect the collision frequency. The inability to discern effects of ligand binding with this broadening agent may be due to either the larger size or the negative charge, or to both, but is no evidence of major changes in accessibility of Cys-674 to this reagent.

DISCUSSION

It is evident that Cys-674 is uniquely reactive with ISl, and that the reactivity of this side chain increases when substrate and Ca^{2+} are bound to the enzyme. It is further evident that 4 nmol/mg Cys is preferentially labeled by IAF under these conditions, and comparisons to samples that have been prelabeled with ISL indicate that this too is Cys-674. If the reactivity of another side chain had been increased by addition of substrate, a residual fast group should have been apparent in the time course of the enzyme prelabeled with ISL (Figure 3b). Bishop et al. (1988) did not publish time courses for the IAF reaction; however, our results are consistent with their observation that IAF reacts with Cys-670. Our time courses also show evidence of slower reacting side chains of indeterminate number. The relatively slow reaction rate of IAF with what appears to be Cys-674 and Cys-670 may be responsible for this lack of resolution.

Kawakita and co-workers measured time courses with IAF, as well as with [^{14}C]iodoacetamide and IAEDANS (Baba et al., 1986), and the results with IAF were similar to those observed here. [^{14}C]Iodoacetamide behaved in a manner similar to IAF (a slow reaction rate without an apparent leveling of the time course), while the reaction with IAEDANS was similar to our results with ISL. Both IAEDANS and iodoacetamide were reported to be primarily on Cys-674. Kawakita and cohworkers did not obtain time courses with substrate and Ca^{2+} bound to the enzyme, although they noted evidence of a conformational change in the IAEDANS spectrum. Considering the consistency of the data, it is likely that IAEDANS and iodoacetamide would demonstrate the increased reactivity that we observe with ISL and IAF when substrate and Ca^{2+} are present, and that limited amounts of label could be directed to Cys-674 with all these derivatives when labeled in the manner of sample A.

The question then arises as to why Cys-674 has such high reactivity with iodoacetamide derivatives, and why ISL is more selective than IAF. Here we have been able to determine that Cys-674 has a low pK, which would certainly make it more reactive at pH 6.8 than other Cys residues. It also appears that this residue is in a highly constricted region, such as a crevice or a hydrophobic pocket. The quenching experiments described in Figures 8 and 9 should be quite sensitive to the accessibility of the labeled residue, and the amount of protection, observed in all cases except for the partial accessibility to Ni^{2+}, is considerable. The iodoacetamide derivatives with hydrophobic rings would be directed toward a hydrophobic site. Furthermore, if the section of the peptide backbone containing Cys-674 is part of a crevice or fold in the structure, then it would not be surprising if the two other Cys side chains in this region, Cys-675 and Cys-670, were oriented in such a manner as to be inaccessible. Cys-675 is at the beginning of a segment that Green and co-workers predict to be a β strand (Brandl et al., 1986), and Bishop and co-workers (1988) suggested that this side chain may be folded back into the structure. These researchers also suggested that the large size of IAF might cause some opening of the structure, exposing Cys-670.

There are several properties of the derivatives that could affect their selectivity, including hydrophobicity, size, polarizability, and charge. ISL is the only one of these derivatives, other than iodoacetamide, that is not charged and is not aromatic. However, it is hydrophobic (the water solubility is considerably lower than that of IAEDANS and only slightly higher than that of IAF) but, in contrast to IAF, has no measurable solubility in the SR lipids. It contains only one hydrocarbon ring, and is considerably smaller than IAF or IAEDANS. IAEDANS is not only larger than ISL, but contains a two-carbon chain between the rings and the iodoacetamide. Thus, the best explanation for the higher selectivity of ISL may be the combination of its hydrophobic nature and its relatively compact size.

The major use of ISL has been as a probe for conformational changes that accompany substrate binding, and the effect that Ca^{2+} binding has on the substrate interactions. Early work, using ATP analogs, suggested that this conformation is one that is related to the formation of an activated complex,

leading directly to phosphorylation (Coan, 1983). Kinetic studies of the ATP hydrolysis mechanism have demonstrated that a major conformational change occurs at precisely this step (Pickart & Jencks, 1982; Petithory & Jencks, 1986), and more recently, time domain measurements of ISL parameters using caged ATP as a substrate have been able to align these data (Lewis & Thomas, 1992; Mahaney et al., 1993). Locating ISL on Cys-674 must mean that this conformational change affects regions of the enzyme that are quite distal from the catalytic site where it originates. The decrease in ISL mobility we observe in the EPR spectrum on substrate binding is consistent with the observed decrease in accessibility to Ni^{2+}, and indicates a general closure of the enzyme around Cys-674. This is also consistent with the increase in reaction rate considering that the hydrophobicity of the site would be increased.

The experiments presented here demonstrate the presence of more than one enzyme conformation under most of the given sets of conditions. The division of the $NiCl_2$ titration into two populations could be due to an increase in solvent accessibility of the small cation to Cys-674, or it could be due to exposure of a site where Ni^{2+} can bind, but it must mean that about 50% of the enzyme is in a different conformation. The reversibility of the spectral parameters on removal and reintroduction of substrate and Ca^{2+} (Figure 5d,e; Coan & Keating, 1982; Coan, 1983) leads to the same conclusion. Rapid kinetic measurements of the rates of E–P formation and Ca^{2+} dissociation at low temperatures have indicated the presence of two nonequivalent functional subunits (Ikemoto et al., 1981), but the structural basis for these observations was difficult to discern at the time. However, when taken with the observations made here and the recent time domain studies on Thomas and co-workers, it would appear that about 50% of the enzyme is in a conformation that more readily utilizes the substrate.

REFERENCES

Anderson, K. W., & Murphy, A. J. (1983) *J. Biol. Chem. 258*, 14276–12378.

Bevington, P. R. (1969) *Data Reduction and Error Analysis for the Physical Sciences*, McGraw-Hill, New York.

Baba, A., Nakamura, T., & Kawakita, M. (1986) *J. Biochem. (Tokyo) 100*, 1137–1147.

Bigelow, D. J., & Inesi, G. (1991) *Biochemistry 30*, 2113–2125.

Bigelow, D. J., Squire, T. C., & Inesi, G. (1992) *J. Biol. Chem. 267*, 6952–6962.

Birmachu, W., Nisswadt, F. L., & Thomas, D. D. (1989) *Biochemistry 28*, 3940–3947.

Bishop, J. E., Squire, T. C., Bigelow, D. J., & Inesi, G. (1988) *Biochemistry 27*, 5233–5240.

Brandl, C. J., Green, N. M., Korczak, B., & MacLennan, D. H. (1986) *Cell 44*, 597–607.

Champeil, P., Buschlen-Boucly, S., Bastide, F., & Gary-Bobo, C. (1978) *J. Biol. Chem. 253*, 1179–1186.

Chen, Z., Coan, C., Fielding, L., & Cassafer, G. (1991) *J. Biol. Chem. 266*, 12366–12394.

Clarke, D. M., Loo, T. W., Inesi, G., & MacLennan, D. H. (1989) *Nature 339*, 476–478.

Clarke, D. M., Maruyama, K., Loo, T. P., Leberer, E., Inesi, G., & MacLennan, D. H. (1989) *J. Biol. Chem. 264*, 11246–11251.

Coan, C. (1983) *Biochemistry 22*, 5826–5834.

Coan, C. (1985) *J. Biol. Chem. 260*, 8134–8144.

Coan, C. R., & Inesi, G. (1977) *J. Biol. Chem. 252*, 3044–3049.

Coan, C., & Keating, S. (1982) *Biochemistry 21*, 3214–3220.

Coan, C., Verjovski-Almeida, S., & Inesi, G. (1979) *J. Biol. Chem. 254*, 2968–2974.

Dalal, D. P., Damoder, R., Benner, C., Eaton, G. R., & Eaton, S. S. (1985) *J. Magn. Reson. 63*, 125–132.

Dupont, Y. (1976) *Biochem. Biophys. Res. Commun. 71*, 544–550.

Eletr, S., & Inesi, G. (1972) *Biochim. Biophys. Acta 282*, 174–179.

Fernandez-Belda, F., Kurzmak, M., & Inesi, G. (1984) *J. Biol. Chem. 259*, 9687–9698.

Highsmith, S., & Murphy, A. J. (1984) *J. Biol. Chem. 259*, 14651–14656.

Ikemoto, N., Garcia, A. M., Kurobe, Y., & Scott, T. L. (1981) *J. Biol. Chem. 256*, 8593–8601.

Imamura, Y., Saito, K., & Kawakita, M. (1984) *J. Biochem. (Tokyo) 95*, 1305–1313.

Inesi, G., Sumbilla, C., & Kirtley, M. E. (1990) *Physiol. Rev. 70*, 749–760.

Inesi, G., Kurzmack, M., Coan, C., & Lewis, D. (1980) *J. Biol. Chem. 255*, 3025–3031.

Jencks, W. P. (1989) *J. Biol. Chem. 264*, 18855–18858.

Keith, A. D., Snipes, W., Mehlhorn, R. J., & Gunter, T. (1977) *Biophys. J. 19*, 205–218.

Kurtenbach, E., & Verjovski-Almeida, S. (1985) *J. Biol. Chem. 260*, 9636–9642.

Laemmli, U. K. (1970) *Nature 227*, 680–685.

Lewis, S. M., & Thomas, D. D. (1992) *Biochemistry 31*, 7381–7389.

Lowry, O., Rosenbrough, N., Farr, A., & Randell, R. (1951) *J. Biol. Chem. 193*, 265–275.

MacLennan, D. H. (1990) *Biophys. J. 58*, 1355–1365.

Mahaney, J. E., Froehlich, J. P., & Thomas, D. D. (1993) *Biophys. J. 64*, A305.

Miki, K., Scott, T. L., & Ikemoto, N. (1981) *J. Biol. Chem. 256*, 9382–9385.

Mitchinson, C., Wilderspin, A. F., Trinnaman, B. J., & Green, N. M. (1982) *FEBS Lett. 146*, 87–92.

Murphy, A. J. (1976) *Biochemistry 15*, 4492–4496.

Murphy, A. (1978) *J. Biol. Chem. 253*, 385–389.

Petithory, J. B., & Jencks, W. P. (1986) *Biochemistry 25*, 4493–4497.

Pickart, C. M., & Jencks, W. P. (1982) *J. Biol. Chem. 257*, 5319–5322.

Scott, T. L. (1985) *J. Biol. Chem. 260*, 14421–14423.

Squire, T. C., Bigelow, D. J., de Ancos, J. G., & Inesi, G. (1987) *J. Biol. Chem. 262*, 4748–4754.

Suzuki, H., Obara, M., Kuwayama, H., & Kanazawa, T. (1987) *J. Biol. Chem. 262*, 15488–15456.

Taylor, W. R., & Green, N. M. (1989) *Eur. J. Biochem. 179*, 241–248.

Thorley-Lawson, D. A., & Green, N. M. (1973) *Eur. J. Biochem. 40*, 403–413.

Yager, T. D., Eaton, G. R., & Eaton, S. S. (1979) *Inorg. Chem. 18*, 725–727.

Yamashida, T., & Kawakita, M. (1987) *J. Biochem (Tokyo) 101*, 377–385.